Enhancement of Thermal Stability Associated with the Chemical Treatment of Bacterial (*Gluconacetobacter xylinus*) Cellulose

Johnsy George, V. A. Sajeevkumar, R. Kumar, K. V. Ramana, S. N. Sabapathy, A. S. Bawa

Food Engineering and Packaging, Defence Food Research Laboratory, Siddarthanagar, Mysore 570011, Karnataka, India

Received 17 August 2007; accepted 13 November 2007
DOI 10.1002/app.27802
Published online 29 January 2008 in Wiley InterScience (www.interscience.wiley.com).

ABSTRACT: Bacterial cellulose produced by *Gluconacetobacter xylinus* was treated with sodium carbonate (Na_2CO_3) and sodium hydroxide (NaOH) to remove entrapped noncellulosic materials. Fourier transform infrared (FTIR) spectroscopy has been used to investigate the effect of alkali on the chemical structure of bacterial cellulose. The changes in the crystalline nature of these membranes were analyzed using X-ray diffraction (XRD) technique. The morphology and the removal of noncellulosic impurities followed by alkali treatment were studied using scanning electron microscopy (SEM) and energy dispersive X-ray spectrometry (EDS). The enhanced thermal stability of bacterial cellulose was evident from thermogravimetric analysis (TGA). Further, the alkali treatments resulted in relatively pure form of cellulose, which finds application in various spheres. © 2008 Wiley Periodicals, Inc. J Appl Polym Sci 108: 1845–1851, 2008

Key words: FT-IR; X-ray; thermogravimetric analysis; activation energy

INTRODUCTION

Among the bacteria, *Gluconacetobacter xylinus* synthesizes cellulose in the form of floating pellicle in growth medium, under static culture conditions. The pellicle is processed by alkali treatment to obtain a relatively pure form of cellulose. The bacterial cellulose is superior to plant cellulose owing to its purity and nanomorphology in combination with a variety of properties such as high water holding capacity,[1] large surface area, elasticity, mechanical strength, and biocompatibility.[2] The material is expected to play a major role as food additive, as a scaffold in tissue engineering,[3] food packaging,[4] and preparation of composite materials.[5] Alkali treatment of bacterial cellulose is of considerable importance, as it converts native cellulose into pure cellulose by removing entrapped noncellulosic materials like protein, nucleic acid, and other media debris.

The crystal structure, morphology, and thermal stability of bacterial cellulose can vary, depending on the concentration of alkali and hydrothermal treatment employed. The molecular arrangement of cellulose, formed by hydrogen bond network between hydroxyl groups can also be affected by such alkali treatments. FTIR spectroscopy is a convenient method for elucidating structure, crystallinity, and nature of intermolecular/interchain hydrogen bonding and other physical properties of cellulose.[6] X-ray diffraction analysis of native cellulose suggests the existence of cellulose I as a monoclinic unit cell containing cellulose chains in parallel orientation.[7] Thermodynamically less stable cellulose I can convert into more stable cellulose II form during mercerization or dissolution of cellulose.[8] This type of conversion from one crystal structure to other can change the properties of cellulose. Other characteristic properties of cellulose like hydrophilicity, chirality, biodegradability, etc. depend on the morphology, which can vary with molecular hierarchy of elementary fibrils, microfibrils, and microfibrillar bands.[9]

Thermal stability of bacterial cellulose is of prime importance, for its applications involving higher temperatures. Thermal decomposition of cellulose involves both dehydration and depolymerization that result in the formation of solid residues, high boiling volatiles, and gaseous products,[10] which can be effectively studied using TGA. Although thermal decomposition of plant and other celluloses from biomass is well documented under different conditions,[11] information on bacterial cellulose is scarce. In our previous investigations, we have reported certain physical, chemical,[12] and thermal[13] properties of alkali treated bacterial cellulose. In the present work, we have attempted to utilize the FTIR and X-ray diffraction analysis to assess the changes that take place in the crystallinity of bacterial cellulose during alkali treatments. The morphological changes occurring as a result of alkali treatment were studied using SEM and the purity of resulted membranes was

Correspondence to: J. George (g.johnsy@gmail.com).

investigated using EDS analysis. The thermal stability of the treated membranes was studied using TGA, followed by the estimation of activation energy required for the thermal decomposition using Flynn-Wall-Osawa method.

EXPERIMENTAL

Biosynthesis and treatment of cellulose membranes

The Gluconacetobacter xylinus strain used in the study was the same as reported in our previous study.[12] The bacterial culture was maintained in a solid medium with same composition reported earlier.[14] The liquid medium with same composition was used for the production of cellulose under static culture conditions over a period of 2 weeks at 30°C to 35°C, by the organism. The cellulose obtained in the form of pellicles was treated with 0.2*N* $NaOH/Na_2CO_3$ solutions, by boiling for 30 min followed by extensive washing with distilled water, till the complete removal of alkali as confirmed by the neutral pH of drained water. The treated membranes were dried between filter papers at 60°C for 10–12 h. These dried membranes of uniform thickness, prepared from the same batch were used for further analysis.

Fourier transform infrared spectroscopic analysis

The native as well as alkali treated cellulose were analyzed by Fourier transform infrared (FTIR) spectroscopy. The IR spectra were recorded using Thermo Nicolet FTIR spectrometer (Model 5700, Madison, WI) fitted with single bounce Attenuated Total Reflectance (ATR) accessory with ZnSe crystal. Efforts were made to provide same pressure to all samples using the pressure device attached to the accessory. Sixty-four scans were averaged to reduce the noise. All spectra were recorded at 4 cm^{-1} resolution and analysis of the spectra was carried out using the software provided along with the instrument.

X-ray diffraction analysis

X-ray diffraction (XRD) studies were conducted using a Bruker (DS Discover, Madison, WI) X-ray diffractometer. The diffraction patterns were recorded using Cu-Kα radiation having λ of 1.54060 Å. The samples taken in the form of membranes were analyzed over a scanning range of $2\theta = 1–40°$.

Scanning electron microscopy and energy dispersive X-ray spectrometry

Scanning electron micrographs (SEM) were obtained using a FEI (Nova nanosem 600) Field emission SEM (Netherlands). All images were taken at low vacuum using an operating voltage of 5 kV. Energy dispersive X-ray spectrometry (EDS) analysis was conducted using an EDS attachment connected to the SEM.

Thermogravimetric analysis

Thermogravimetric analyzer (TGA Q 50, TA Instruments, New Castle, DE) was employed in conjunction with a thermal analysis controller, to measure the rate of weight loss of cellulose material as a function of temperature and time in a controlled atmosphere. About 10 mg of cellulose was kept in a platinum crucible and heated in a furnace, flushed with N_2 gas at the rate of 40 mL/min. The samples were heated from 30°C to 600°C at different heating rates. The percentage weight loss and derivative weight loss were recorded against temperature for all samples. Thermogravimetric measurements together with Flynn-Wall-Osawa approach have been employed to assess the kinetic parameters to compare the thermal behavior of native and alkali treated cellulose.

RESULTS AND DISCUSSION

Fourier transform infrared spectroscopy

Cellulose is a biopolymer comprising of β-D-glucopyranose units linked together through β-(1,4) glycosidic linkages, which can be characterized by FTIR spectroscopy. FTIR is a useful tool in revealing chemical structure and changes in the crystallinity of bacterial cellulose. Figure 1 depicts the FTIR spectra of native, Na_2CO_3, and NaOH treated cellulose membranes, respectively, recorded using single bounce ATR accessory systems. A broad absorptive band observed between 3700 cm^{-1} and 3000 cm^{-1} corresponds to the —OH stretching vibrations of cellulose and water molecules. This may also have contribution

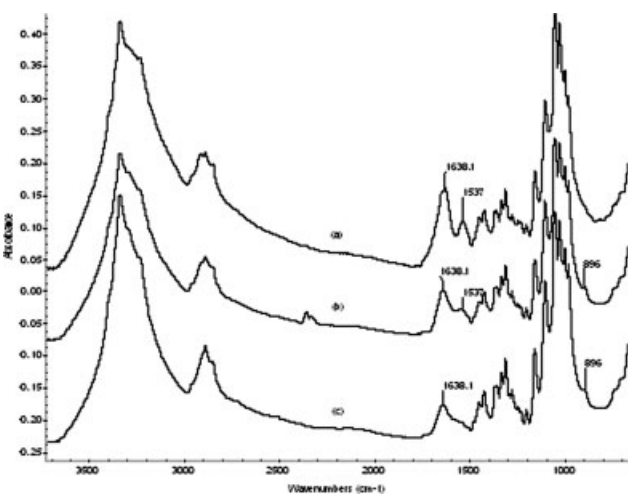

Figure 1 FTIR spectra for (a) native, (b) Na_2CO_3 treated, and (c) NaOH treated bacterial cellulose.

from N—H stretching vibration of amide groups due to the biological impurities present in bacterial cellulose. The peak around 1640 cm^{-1} is due to the H—OH bending vibration of adsorbed water molecules in cellulose.[15] The C—H stretching vibration bands of $—CH_3$ and $—CH_2$ groups are observed as a broad band centered at 2893 cm^{-1}, while bending bands of these groups are noticed at 1426, 1368, 1335, and 1314 cm^{-1}.[16,17] The region between 1000 cm^{-1} and 1200 cm^{-1} has shown several bands in the fingerprint region of native cellulose. The band at 1160 cm^{-1} corresponds to the C—C stretching, which is the asymmetric ring breathing mode while at 1107 cm^{-1} corresponds to glycosidic C—O—C stretching vibration. The bands at 1055 cm^{-1} and 1031 cm^{-1} correspond to the C—OH stretching vibration of secondary and primary alcohols of cellulose, respectively. The observation of these bands confirms the presence of cellulose in the membranes and is in agreement with band assignments reported earlier.[18] The main difference observed in the spectra of native and alkali treated membranes is the presence of a band at 1537 cm^{-1}, which corresponds to amide II band of proteins and other biological impurities in native cellulose. During mild alkali treatment with Na_2CO_3, the amide II band was found to decrease in intensity and was found to disappear on treatment with strong alkali like NaOH. The broad band from 3700 cm^{-1} to 3000 cm^{-1} of native cellulose tends to become narrow after alkali treatment. This could be because of the removal of amide groups present in biological impurities during alkali treatment. Ping et al.[19] reported that broad —OH stretching vibration bands at around 3250 cm^{-1} in hydrophilic polymers show variation depending on the chemical nature of polar sites available. The presence of amide groups in noncellulosic contaminants can also retain more water molecules through intermolecular hydrogen bonding resulting in the broad —OH band of the native cellulose. Hence removal of such impurities from bacterial cellulose by alkali treatments decreases N—H stretching of amide groups as well as H-bonding and subsequently narrowing the broad band from 3700 cm^{-1} to 3000 cm^{-1}. This is also evident from the decrease in intensity of H—O—H bending vibration of adsorbed water at 1638 cm^{-1} during alkali treatments. After alkali treatments, a new band centered on 896 cm^{-1} started emerging. Dinand et al.[20] have assigned a band near 895 cm^{-1} as the conversion of native cellulose (cellulose I) to cellulose II allomorph. A similar phenomenon was noticed with the bacterial cellulose after alkali treatments.

X-ray diffraction analysis

Electron diffraction experiments proved that native cellulose exists predominantly in the form of cellulose I crystalline structure.[21] The XRD patterns of native cellulose obtained in our experiments (Fig. 2) was identified with characteristic peaks at $2\theta = 14.8$, 17.2, and 22.6 along with two other peaks at 9.6 and 28.4. After alkali treatments the peaks at 9.6 and 28.4 disappeared, which is the indication of removal of noncellulosic materials by alkali treatments. Alkali treatment also affected the diffraction pattern corresponding to $(1\bar{1}0)$, (110) and (200) planes in the native cellulose. A rise in relative intensity of peak, corresponding to (200) plane in comparison with that of $(1\bar{1}0)$ plane, as well as a shift in the peak position of (200) plane toward lower angle was observed. A peak corresponding to (200) plane at $2\theta = 21.6$ indicates the presence of cellulose II allomorph.[22] Increase in the relative intensity of (200) plane diffraction and its shift may be due to the increased amount of cellulose II in alkali treated membranes, which is also supported by the observations made in FTIR analysis. Also the $(1\bar{1}0)$ and (110) reflections in alkali treated cellulose are positioned closer together compared to that of native cellulose. These changes in the *d*-spacing appear to represent a change in the proportion of cellulose allomorphs and hence it may be concluded that thermodynamically less stable cellulose I is getting converted to a more stable form of cellulose II after alkali treatments.

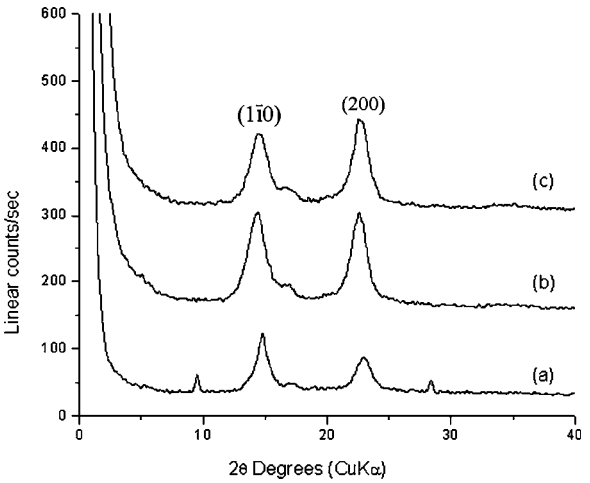

Figure 2 X-ray diffraction pattern of (a) native, (b) Na_2CO_3 treated, and (c) NaOH treated bacterial cellulose.

Scanning electron microscopy and energy dispersive X-ray spectrometry

The distinct fiber morphology of cellulose is responsible for its unique properties and applications. Scanning electron micrographs of native cellulose as shown in Figure 3, implies the existence of noncellulosic impurities entangled with cellulose fibrils. Alkali treatments were effective in removing most of the noncellulosic impurities from the cellulose matrix,

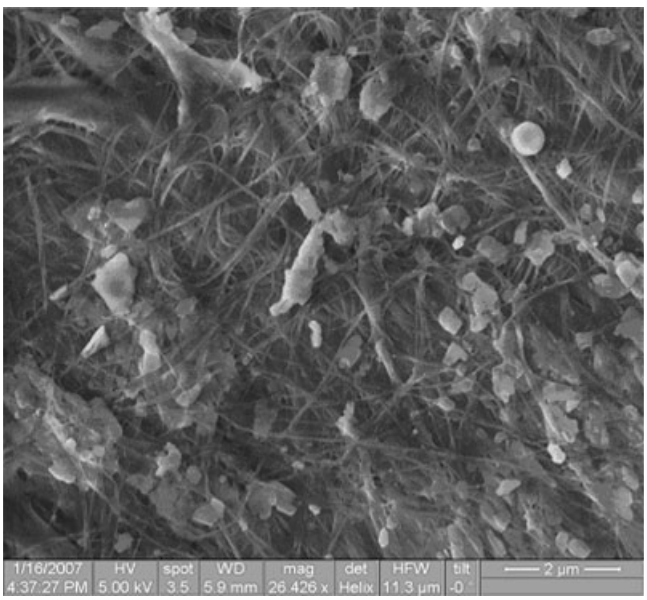

Figure 3 Scanning electron micrographs of native cellulose.

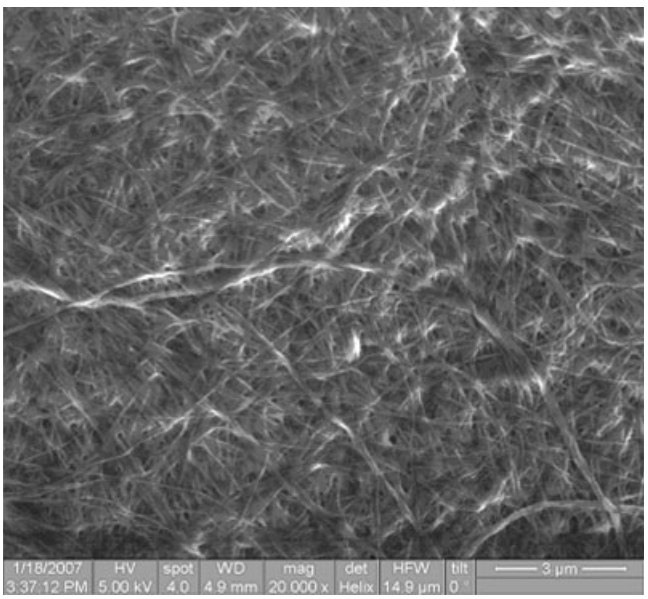

Figure 5 Scanning electron micrographs of NaOH treated bacterial cellulose.

even though some traces of residual impurities were observed in the case of Na_2CO_3 treated membranes (Figs. 4 and 5). EDS analysis of native cellulose [Fig. 6(a)] shows the presence of elements like sodium, potassium, phosphorous, and sulfur, which are commonly present in biological samples like proteins and nucleic acids along with carbon and oxygen elements of cellulose. The effect of Na_2CO_3 and NaOH on native cellulose is evident in EDS analysis [Fig. 6(b,c)], which shows the absence of elements corresponding to the biological impurities and thereby confirming that alkali treatments are effective in obtaining a relatively pure form of bacterial cellulose.

Thermogravimetric analysis

On heating, the bacterial cellulose decomposes at temperatures above 250°C, leading to the formation of volatiles, low molecular weight polysaccharides and carbonaceous char. Understanding the mechanism of thermal decomposition is essential for optimizing its processing conditions at elevated

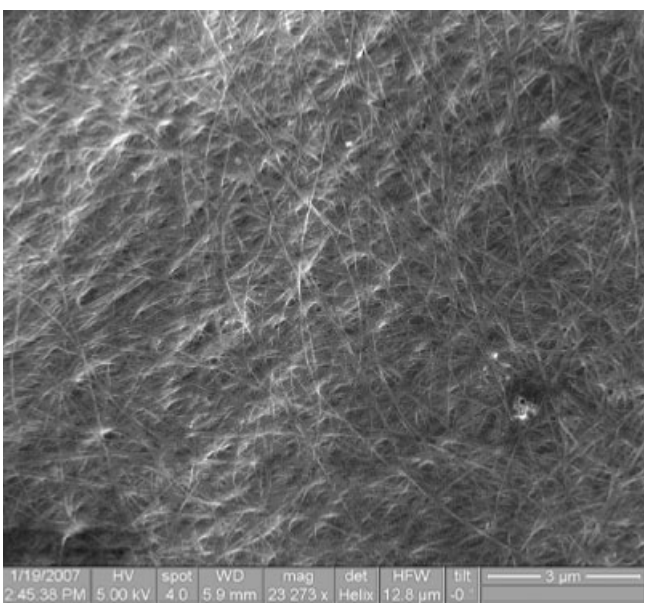

Figure 4 Scanning electron micrographs of Na_2CO_3 treated bacterial cellulose.

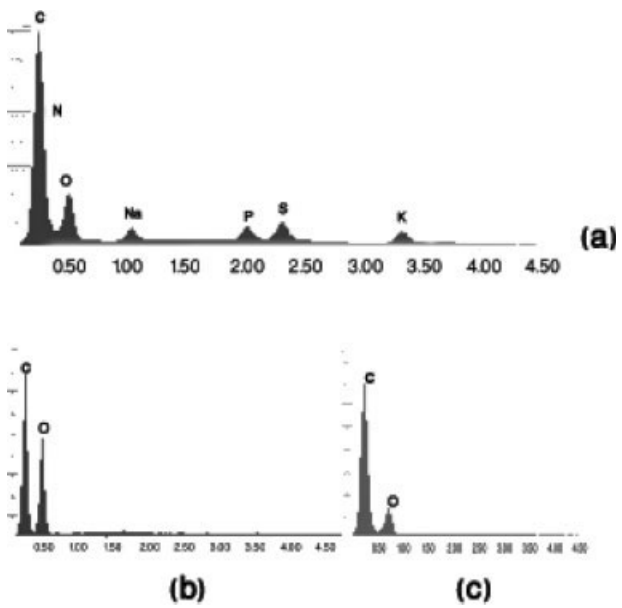

Figure 6 EDS spectra of (a) native, (b) Na_2CO_3 treated, and (c) NaOH treated bacterial cellulose.

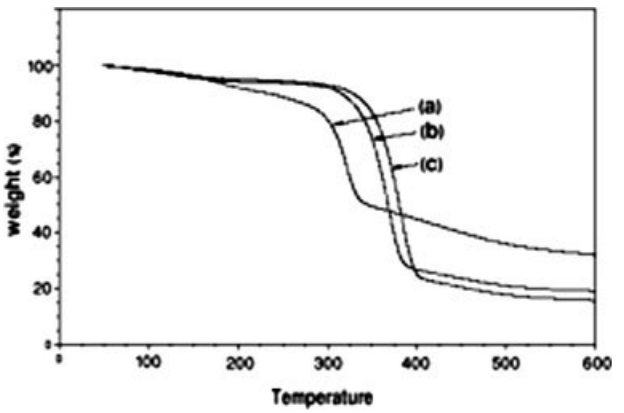

Figure 7 TGA curves of (a) native, (b) Na_2CO_3 treated, and (c) NaOH treated bacterial cellulose at a heating rate of 20°C/min.

temperatures. The temperature of initial cellulose decomposition is an indication of the highest operating temperature for its application. Thermogravimetric analysis, which measures the weight loss during heating, represents the thermal stability and degradation pattern of cellulosic materials. In our earlier investigation,[13] we have reported variations in thermal properties of native and alkaline treated cellulose. In this study, our aim is to explain the factors contributing to the improved thermal stability of alkali treated bacterial cellulose and to determine the activation energy of cellulose decomposition. Figure 7 depicts the TGA curves of native, Na_2CO_3, and NaOH treated cellulose membranes, which clearly suggests that the thermal decomposition pattern changes completely after alkali treatments. It is known that the relative ratios of main pyrolysis products of biomass including cellulose are strongly influenced by the physical and chemical characteristics of the raw materials. In our investigations, we found that the alkali treatments employed for removing proteinaceous and other impurities from the bacterial cellulose enhanced its thermal stability by way of an increase in decomposition temperature. The bacterial cellulose in its native form is highly crystalline and exists as a system in which microfibrils of opposite polarity coexist side by side within the self assembled ribbons present on cellulose I allomorph. Native cellulose on mercerization and subsequent washing, cellulose I (parallel form) will be converted into a more thermally stable form of antiparallel cellulose II.[23] A similar phenomenon was observed in our investigation, which is confirmed through FTIR studies and XRD studies. This conversion mechanism occurring during alkali treatments may be the reason for higher thermal stability shown by the treated cellulose. Thermal decomposition pattern of cellulose can be explained mainly by two different mechanisms.[24] The first was dominant at temperatures <300°C, while second mechanism was prevalent at temperatures > 300°C. The first mechanism involves the degradation by breaking of internal bonds, dehydration, formation of free radicals, and reactive carbonaceous char. The second mechanism involves the cleavage of secondary bonds and formation of intermediate products such as anhydromonosaccharides, which are converted into low molecular weight polysaccharides and finally carbonized products.[25] The char and tar formation during cellulose degradation is influenced by the mechanism through which degradation occurs. In the case of native cellulose, the degradation of cellulose can be initiated at temperatures lower than 300°C, and continues with further temperature. As a result, the degradation can be considered as a combination of both mechanisms leading to the formation of more carbonaceous char, whereas in alkali treated cellulose, the decomposition started at above 300°C according to second mechanism resulting in lower char yield. To determine the activation energy of thermal decomposition for bacterial cellulose, Flynn-Wall-Osawa method was followed for a nonisothermal TGA of the cellulose at five different, constant heating rates of 2°C/min, 5°C/min, 10°C/min, 15°C/min, and 20°C/min. The decomposition temperature was found to depend on the rate of heating. From the DTG curves (Figs. 8, 9, and 10) it is evident that with an increase in heating rate, the shift in thermograms toward higher temperatures can takes place. This phenomenon can be explained as, at lower heating rates, the time for which the material was exposed to a particular temperature was more and hence more degradation occurred even at lower temperatures.

The log β versus $10^3/T$ was plotted for different conversion levels starting from 10 to 90%. Figure 11 depicts the plots for native, Na_2CO_3, and NaOH treated cellulose, respectively. The straight lines obtained for native cellulose up to 20% conversion

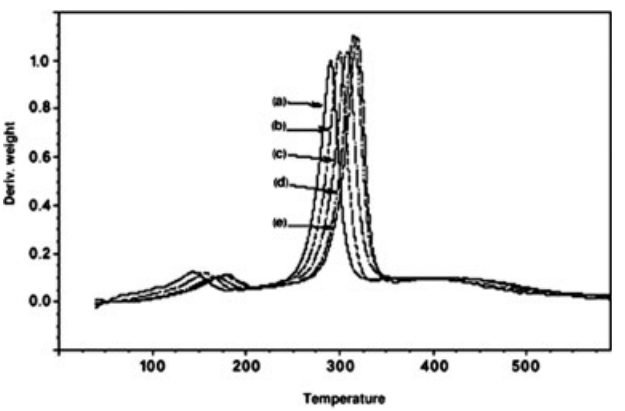

Figure 8 DTG curves of native cellulose at different heating rates (a) 2°C/min, (b) 5°C/min, (c) 10°C/min, (d) 15°C/min, and (e) 20°C/min.

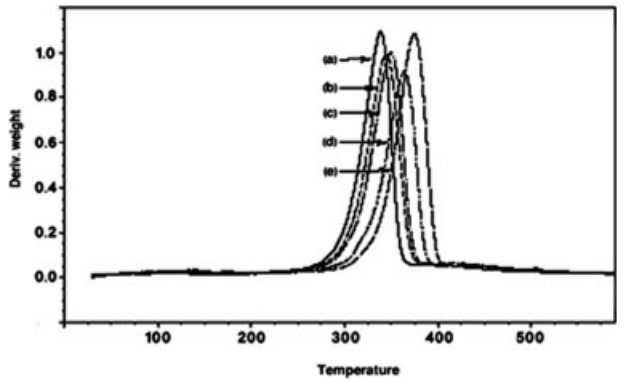

Figure 9 DTG curves of Na_2CO_3 cellulose at different heating rates (a) 2°C/min, (b) 5°C/min, (c) 10°C/min, (d) 15°C/min, and (e) 20°C/min.

were not as parallel as alkali treated cellulose and were more broadly spaced. This can be attributed to the presence of impurities that varied from 15 to 20%, since the degradation pattern of these impurities and that of the cellulose was different. In the case of alkali treated cellulose, the NaOH treated membranes showed more uniform pattern proving the ability of strong alkali to remove unwanted debris from the membrane, with further evidence emerging from the FTIR and SEM analysis. After 20% conversion levels these lines were parallel and narrowly spaced up to 70%. In case of native cellulose and alkali treated membranes, almost parallel and uniform plots were seen for conversions in the range of 10–80%. This region corresponds to the degradation of cellulose while the eventual char formation is influencing the degradation kinetics in the remaining conversion regions. The cumulative values for activation energy (Ea) were calculated from the log β versus $1000/T$ graph and plotted against percentage conversion levels (Fig. 12). Activation energy required for thermal decomposition depended on the energy barrier preventing the decomposition of polymer and is influenced by the purity and chemical treatment given to the bacterial cellulose. Native cellulose required lower Ea for thermal decomposition, followed by Na_2CO_3 and NaOH treated ones. The activation energy plot for native cellulose exhibits three distinct stages. The first stage from 0 to 20% conversion levels showed a rapid increase in the activation energy. The Ea values up to 20% conversion levels are significantly lower and mostly attributed to the degradation of biological impurities with comparatively lower thermal stability. The native cellulose has 14–18% of

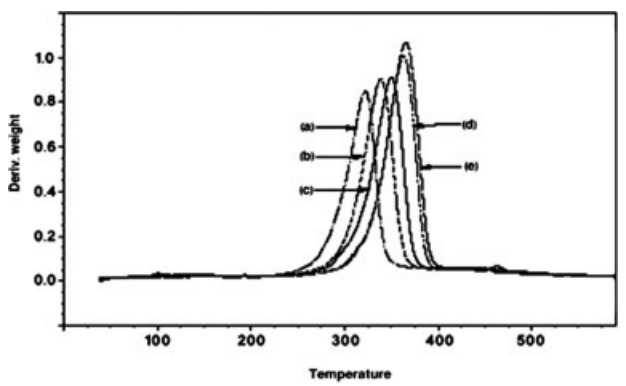

Figure 10 DTG curves of NaOH cellulose at different heating rates (a) 2°C/min, (b) 5°C/min, (c) 10°C/min, (d) 15°C/min, and (e) 20°C/min.

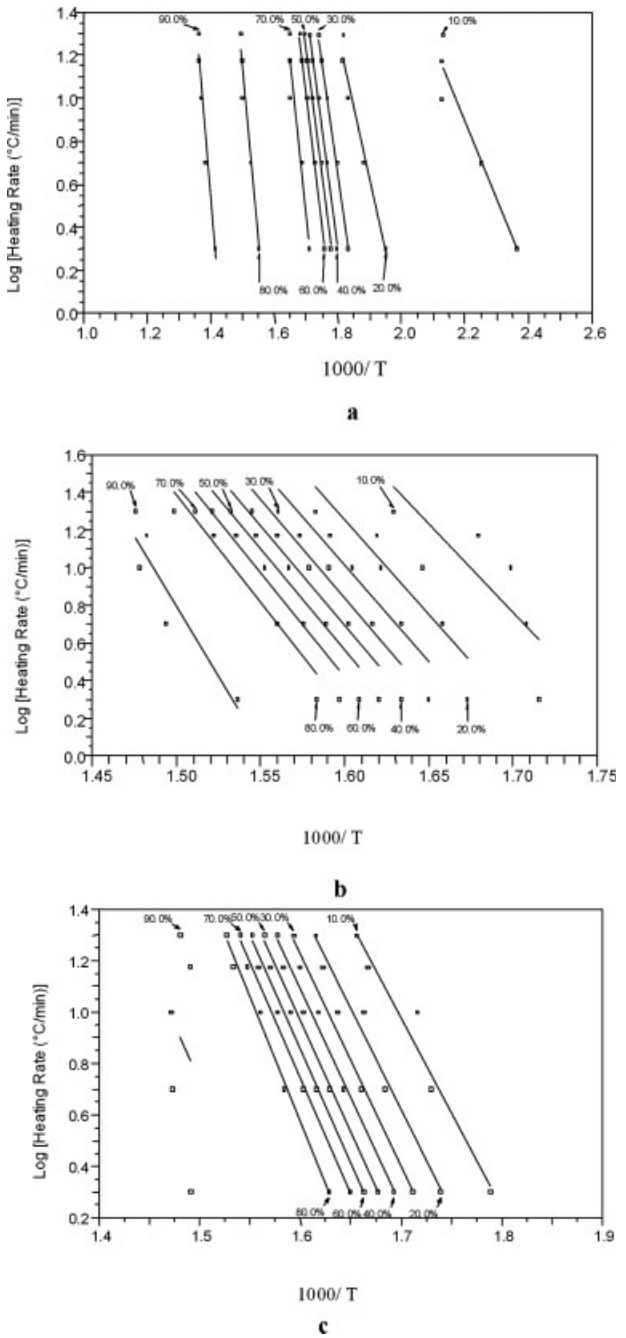

Figure 11 Log β versus $1000/T$ plot of (a) native, (b) Na_2CO_3 treated, and (c) NaOH treated bacterial cellulose.

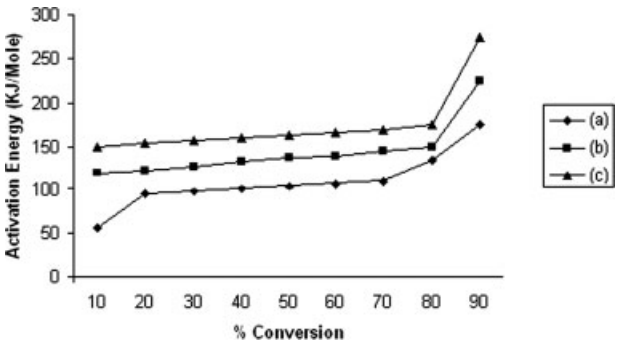

Figure 12 Activation energy versus % conversion plots of (a) native, (b) Na_2CO_3 treated, and (c) NaOH treated bacterial cellulose.

proteins and 1–1.25% of nucleic acids as reported earlier.[13] In addition, the increase in Ea values suggested the decomposition of relatively small amount of cellulose in this region. In the second stage (from 20 to 70%), the activation energy found to increase steadily, which can be attributed to degradation of cellulose. The third stage (from 70 to 90%) showed a rapid increase in the activation energy where charring was also found to occur. The charring process is an endothermic step[26] and hence more activation energy is recorded. The gradual increase in activation energy at the second stage is an indication of char formation even at low temperatures, suggesting the native cellulose degradation by a combination of two different mechanisms. In the case of Na_2CO_3 and NaOH treated cellulose, Ea values were almost constant from 10 to 80% conversion levels indicating the absence of any impurity at levels greater than 10% in the alkali treated cellulose, there after the char formation was initiated, resulting in a steep increase in Ea values. These results provide an insight into the factors, which can affect the activation energy during the decomposition of bacterial cellulose.

CONCLUSIONS

Bacterial cellulose, a natural polymer with its unique properties, is superior to plant cellulose and can be used as a reasonable substitute for various nonbiodegradable synthetic polymers for large-scale industrial and specialty applications. The alkali treatments commonly employed in the process of obtaining pure cellulose facilitated the conversion of cellulose I to cellulose II. The alkali treatment was found to be advantageous in enhancing the thermal stability of the material. The thermal decomposition temperature is influenced by the rate of heating, nature of alkali and the percentage purity of bacterial cellulose. The entrapped noncellulosic materials comprising of trace amounts of proteins, nucleic acids, and bacterial cell wall components, conspicuously exerted a strong influence on various steps in the degradation process as well as the activation energies of thermal degradation process of the material. The data obtained delineates the factors influencing thermal degradation of bacterial cellulose, emphasizing the usefulness of the alkali treated bacterial cellulose relatively free from noncellulosic materials, for applications at high temperatures.

The authors are thankful to staff of Central Instrumentation Facility, DFRL and JNCASR, Bangalore, for their valuable help during the study.

References

1. Seifert, M.; Hesse, S.; Kabrrelian, V.; Klemn, D. J Polym Sci Part A: Polym Chem 2004, 42, 463.
2. Backdahl, H.; Helenius, G.; Bodin, A.; Nannmark, U.; Johansson, B. R.; Bisberg, B.; Gatenholm, P. Biomaterials 2006, 27, 2141.
3. Svensson, A.; Nicklasson, E.; Harrah, T.; Panilaitis, B.; Kaplan, D. L.; Brittberg, M.; Gatenholm, P. Biomaterials 2005, 26, 419.
4. Weber, C. J.; Haugaard, V.; Festersen, R.; Bertelsen, G. Food Addit Cont 2002, 19, Suppl 1, 172.
5. Bodhibukkana, C.; Srichana, T.; Kaewnopparat, S.; Tangthong, N.; Bovking, P.; Martin, G. P.; Svedee, R. J Contr Release 2006, 113, 43.
6. Kondo, T. Cellulose 1997, 4, 281.
7. Gardner, K. H.; Blackwell, J. Biopolymers 1974, 13, 1975.
8. Yu, X.; Atalla, R. H. Int J Biol Macromol 1996, 19, 145.
9. Klemm, D.; Heublein, B.; Fink, H. H. P.; Bohn, A. Ang Chem Int Ed Engl 2005, 44, 3358.
10. Shafizadeh, F. J Anal Appl Pyrolysis 1982, 3, 283.
11. Szabo, P.; Varhegyi, G.; Till, F.; Faix, O. J Anal Appl Pyrolysis 1996, 36, 179.
12. George, J.; Ramana, K. V.; Sabapathy, S. N.; Bawa, A. S. W. J Microbiol Biotechnol 2005, 21, 1323.
13. George, J.; Ramana, K. V.; Sabapathy, S. N.; Jagannath, J. H.; Bawa, A. S. Int J Biol Macromol 2005, 37, 189.
14. Watanabe, K.; Yamanaka, S. Biosci Biotech Biochem 1995, 59, 65.
15. Lojewska, J.; Miskowiec, P.; Lojewski, T.; Proniewicz, L. M. Polym Degrad Stab 2005, 88, 512.
16. Marechal, Y.; Chanzy, H. J Mol Struct 2000, 523, 183.
17. Ali, M.; Emseley, A. M.; Herman, H.; Heywood, R. J. Polymer 2001, 42, 2893.
18. Workman, J, Jr. J Appl Spectrosc Rev 2001, 36(2/3), 139.
19. Ping, Z. H.; Nguyen, Q. T.; Chen, S. M.; Zhou, J. Q.; Ding, Y. D. Polymer 2001, 42, 8461.
20. Dinand, E.; Vignon, M.; Chanzy, H.; Heux, L. Cellulose 2002, 9, 7.
21. Sugiyama, J.; Vuong, R.; Chanzy, H. Macromolecules 1991, 24, 468.
22. Zhang, L.; Ruan, D.; Zhou, J. Ind Eng Chem Res 2001, 40, 5923.
23. Revol, J. F.; Dietrich, A.; Goring, D. A. I. Can J Chem 1987, 65, 1724.
24. Rowell, R. M.; LeVan-Green, S. L. Handbook of Wood Chemistry and Wood Composites; CRC Press; Florida, 2005; p 121.
25. Kawamoto, H.; Murayama, M.; Saka, S. J Jap Wood Soc 2003, 49, 469.
26. Soares, S.; Camino, G.; Levchik, S. Polym Degrad Stab 1995, 49, 375.